

A FINITE-ELEMENT COLLOCATION  
METHOD FOR VARIABLY SATURATED FLOW  
IN TWO SPACE DIMENSIONS

Myron B. Allen  
Carolyn L. Murphy

1986

Journal Article  
WWRC-86-17

In

Water Resources Research

Volume 22, No. 11

October 1986

Myron B. Allen  
Department of Mathematics  
University of Wyoming  
Laramie, Wyoming

Carolyn L. Murphy  
Edwards Air Force Base, California

# A Finite-Element Collocation Method for Variably Saturated Flow in Two Space Dimensions

MYRON B. ALLEN

*Department of Mathematics, University of Wyoming, Laramie*

CAROLYN L. MURPHY

*Edwards Air Force Base, California*

This paper introduces a finite-element collocation technique for solving the equation governing two-dimensional flow in a variably saturated porous medium. The scheme uses a mass-conserving formulation of Richards' equation as the basis for the finite-difference time-stepping method. Collocation in tensor-product spaces of Hermite cubics yields a computationally efficient finite-element approximation of the spatial derivatives. A Newton-like iteration gives a temporally stable implicit scheme. The paper examines two sample problems, including an initial boundary-value problem involving subsurface irrigation.

## 1. INTRODUCTION

This paper presents a finite-element collocation scheme for simulating variably saturated flows in two space dimensions. The scheme is an extension of a mass conserving one-dimensional formulation presented earlier [Allen and Murphy, 1985]. The present exposition gives a complete description of work reported more briefly in the work by Murphy and Allen [1986]. Among the key features of the methodology presented here are (1) the particular piecewise polynomial approximations used to represent the spatial heterogeneities in hydraulic conductivity, moisture content, and specific moisture capacity, and (2) the implementation of a Newton-like iterative scheme that ensures a stable, consistent time-stepping procedure in the presence of strong nonlinearities.

The equation we solve is the two-dimensional Richards [1931] equation

$$\nabla \cdot [K(\nabla h - \mathbf{e}_z)] - \frac{\partial \theta}{\partial t} = 0 \quad (1)$$

where  $\nabla \equiv \mathbf{e}_x \partial / \partial x + \mathbf{e}_z \partial / \partial z$ , with  $z$  measuring distance above some datum, and  $\mathbf{e}_x$  and  $\mathbf{e}_z$  are the unit vectors in the  $x$  and  $z$  directions, respectively. In this equation,  $h(x, z, t)$  is the pressure head (m);  $K$  stands for the soil's hydraulic conductivity (m/s); and  $\theta$  signifies the moisture content of the soil (dimensionless). Typically, the physics of variably saturated flows dictate that  $K$  and  $\theta$  vary with  $h$ , and the relationships  $K(h)$  and  $\theta(h)$  make (1) strongly nonlinear.

Our presentation is organized as follows. In section 2 we discuss a time differenced, finite-element projection of (1) onto tensor-product spaces of piecewise polynomial interpolating functions. The time-stepping algorithm uses a Newton-like iterative scheme to accommodate the nonlinearities in material properties. Section 3 describes a collocation scheme that in conjunction with the appropriate treatment of boundaries, furnishes algebraic analogs to the differential equation. Section 4 reviews two sample problems, and section 5 discusses our results and conclusions.

## 2. FINITE-ELEMENT FORMULATION

Our first task in numerically solving (1) is to discretize the governing equation. To do this, we first expand the spatial derivatives using the product rule. Then, assuming a uniform temporal grid  $\{0 < \Delta t < 2\Delta t < \dots < n\Delta t < \dots\}$ , we use a backward (implicit) Euler difference scheme to approximate the time derivative. These procedures yield

$$\frac{\partial K^{n+1}}{\partial x} \frac{\partial h^{n+1}}{\partial x} + \frac{\partial K^{n+1}}{\partial z} \frac{\partial h^{n+1}}{\partial z} + K^{n+1} \left( \frac{\partial^2 h^{n+1}}{\partial x^2} + \frac{\partial^2 h^{n+1}}{\partial z^2} \right) - \frac{\partial K^{n+1}}{\partial z} - \frac{\theta^{n+1} - \theta^n}{\Delta t} \equiv \mathcal{R}(h^{n+1}) = 0 \quad (2)$$

This approximation incurs an  $\mathcal{O}(\Delta t)$  truncation error. For the time being, let us allow the spatial dependencies in (2) to retain their original forms from (1). Equation (2) furnishes an implicit time-stepping scheme for the approximate pressure head  $h^n(x, z) \approx h(x, z, n\Delta t)$ , which we regard as the principal unknown.

To solve (2) (or any spatially discrete analog of it) we must accommodate the dependence of the nonlinear functions  $K^{n+1} = K(h^{n+1})$ ,  $\theta^{n+1} = \theta(h^{n+1})$  on unknown values  $h^{n+1}$  of the pressure head. To do this, we use an iterative method to advance between time levels, solving for iterative increments  $\delta h = h^{n+1,m+1} - h^{n+1,m}$  to progress from the known iteration  $m$  to the next unknown iteration  $m + 1$ . This scheme allows us to lag the nonlinear coefficients by an iteration, giving a linear equation for  $\delta h$ :

$$\left[ -\frac{1}{\Delta t} \frac{d\theta^{n+1,m}}{dh} + K^{n+1,m} \left( \frac{\partial^2}{\partial x^2} + \frac{\partial^2}{\partial z^2} \right) + \frac{\partial K^{n+1,m}}{\partial x} \frac{\partial}{\partial x} + \frac{\partial K^{n+1,m}}{\partial z} \frac{\partial}{\partial z} \right] \delta h = -\mathcal{R}(h^{n+1,m}) \quad (3)$$

where the expression  $\mathcal{R}(h^{n+1,m})$  stands for the quantity

$$-\frac{1}{\Delta t} (\theta^{n+1,m} - \theta^n) + K^{n+1,m} \left( \frac{\partial^2 h^{n+1,m}}{\partial x^2} + \frac{\partial^2 h^{n+1,m}}{\partial z^2} \right) + \frac{\partial K^{n+1,m}}{\partial x} \frac{\partial h^{n+1,m}}{\partial x} + \frac{\partial K^{n+1,m}}{\partial z} \left( \frac{\partial h^{n+1,m}}{\partial z} - 1 \right)$$

and plays a role analogous to that of the residual in standard

Newton schemes. (Indeed, (3) is precisely what we would get using the Newton method for the operator equation  $\mathcal{R}(h^{n+1}) = 0$  in (2) were we to neglect derivatives of  $K(h^{n+1})$  and  $\nabla K(h^{n+1})$  with respect to the unknown  $h^{n+1}$  in computing the Fréchet derivative of the differential operator  $\mathcal{R}$ .) In the sequel we write Equation (3) more compactly as

$$\mathcal{A}^{n+1,m} \delta h = -\mathcal{R}(h^{n+1,m})$$

In executing the iterative method, we begin each time step by setting  $h^{n+1,0} = h^n$  and stop the iteration, setting  $h^{n+1,m+1} = h^{n+1}$ , when  $\|\mathcal{R}(h^{n+1,m})\|_\infty < \varepsilon$  for some prescribed tolerance  $\varepsilon > 0$ .

The formulation leading to (3) differs from standard head-based formulations, which typically use the chain rule to expand the accumulation term as  $\partial\theta/\partial t = (d\theta/dh)\partial h/\partial t$ . Such an expansion calls for the evaluation of the specific moisture capacity  $d\theta/dh$  at some time level in the interval  $[n\Delta t, (n+1)\Delta t]$  in the temporally discrete approximation. There seems to be no simple way of choosing this time level to guarantee global mass conservation in the sense

$$\oint_{\partial\Omega} (K^{n+1} \nabla h^{n+1} - K^{n+1} \mathbf{e}_z) \cdot \mathbf{n} \, dx = \frac{1}{\Delta t} \int_{\Omega} (\theta^{n+1} - \theta^n) \, dx$$

where  $\Omega$  represents the spatial domain of the problem, and  $\mathbf{n}$  is the unit outward normal vector to the boundary  $\partial\Omega$ . It is worth mentioning, however, that Milly [1984] advances an iterative scheme for evaluating  $d\theta/dh$  to force mass conservation. As is discussed in the work by Allen and Murphy [1985], discretizing the flow equation as in (3) avoids this difficulty, allowing iterative updates of all nonlinear flow coefficients simultaneously.

Now let us discretize the time-stepping equation (3) in space. To do this, we project the spatially varying quantities  $h^{n,m}$ ,  $\theta^{n,m}$ ,  $K^{n,m}$  and  $d\theta^{n,m}/dh$  onto finite-element subspaces. For the principal unknown  $h_{n,m}(x, z)$  we select trial spaces spanned by tensor products of piecewise cubic Hermite interpolating functions in the  $x$ - and  $z$ -directions. In one space dimension, denoted generically by  $\zeta$ , the Hermite functions defined on a uniform grid  $\{\zeta_1 < \zeta_2 < \dots < \zeta_L\}$  of mesh  $\Delta\zeta$  are

$$\begin{aligned} H_{0i}(\zeta) &= (\zeta - \zeta_{i-1})^2 [2(\zeta_i - \zeta) + \Delta\zeta] / \Delta\zeta^3 & \zeta \in [\zeta_{i-1}, \zeta_i] \\ H_{0i}(\zeta) &= (\zeta_{i+1} - \zeta)^2 [3\Delta\zeta - 2(\zeta_{i+1} - \zeta)] / \Delta\zeta^3 & \zeta \in [\zeta_i, \zeta_{i+1}] \\ H_{0i}(\zeta) &= 0 & \text{otherwise} \\ H_{1i}(\zeta) &= (\zeta - \zeta_{i-1})^2 (\zeta - \zeta_i) / \Delta\zeta^2 & \zeta \in [\zeta_{i-1}, \zeta_i] \\ H_{1i}(\zeta) &= (\zeta - \zeta_{i+1})^2 (\zeta - \zeta_i) / \Delta\zeta^2 & \zeta \in [\zeta_i, \zeta_{i+1}] \\ H_{1i}(\zeta) &= 0 & \text{otherwise} \end{aligned}$$

As Prenter [1976, chapter 3] demonstrates, these functions give a continuously differentiable interpolation scheme

$$f(\zeta) \approx \sum_{i=1}^L [f(\zeta_i) H_{0i}(\zeta) + f'(\zeta_i) H_{1i}(\zeta)]$$

for functions  $f \in C^1([\zeta_0, \zeta_L])$  whose values and slopes at the nodes  $\zeta_i$  are known.

For tensor-product interpolation on a rectangular region  $\Omega$ , we adopt a two-dimensional grid  $\{x_1 < x_2 < \dots < x_M\} \times \{z_1 < z_2 < \dots < z_N\}$  with nodes (denoted  $\mathbf{x}_i$ ) at the points  $(x_j, z_k)$ . Then, for  $\mathbf{x} \in \Omega$ , we set

$$\delta h(\mathbf{x}) \approx \delta \hat{h}(\mathbf{x}) = \sum_{i=1}^{MN} [\delta_i \varphi_{00i}(\mathbf{x}) + \delta_i^{(x)} \varphi_{10i}(\mathbf{x}) + \delta_i^{(z)} \varphi_{01i}(\mathbf{x}) + \delta_i^{(xz)} \varphi_{11i}(\mathbf{x})] \quad (4)$$

Here  $\delta_i$ ,  $\delta_i^{(x)}$ ,  $\delta_i^{(z)}$ , and  $\delta_i^{(xz)}$  represent approximate values of  $\delta h$ ,  $\partial(\delta h)/\partial x$ ,  $\partial(\delta h)/\partial z$ ,  $\partial^2(\delta h)/\partial x \partial z$ , respectively, at the node  $\mathbf{x}_i$ . The basis functions  $\varphi_{00i}$ ,  $\varphi_{10i}$ ,  $\varphi_{01i}$ , and  $\varphi_{11i}$  are tensor products of the one-dimensional Hermite basis functions;  $\varphi_{pq_i}(\mathbf{x}) = H_{pi}(x)H_{qi}(z)$ . The interpolation error associated with a projection of the form (4) is  $\mathcal{O}(\Delta x^4 + \Delta z^4)$ .

The finite-element projection (4) furnishes a continuously differentiable interpolation scheme for the iterative increment  $\delta \hat{h}$  in which the nodal parameters are unknown except where given by boundary data, as is discussed in the next section. The head  $h$  inherits this interpolation scheme according to the updating rule

$$\begin{aligned} h^{n+1,m+1}(\mathbf{x}) &\approx \hat{h}^{n+1,m+1}(\mathbf{x}) \\ &= \sum_{i=1}^{MN} \{ [(h_i)^{n+1,m} + \delta_i] \varphi_{00i}(\mathbf{x}) + [(h_i^{(x)})^{n+1,m} + \delta_i^{(x)}] \varphi_{10i}(\mathbf{x}) \\ &\quad + [(h_i^{(z)})^{n+1,m} + \delta_i^{(z)}] \varphi_{01i}(\mathbf{x}) \\ &\quad + [(h_i^{(xz)})^{n+1,m} + \delta_i^{(xz)}] \varphi_{11i}(\mathbf{x}) \} \end{aligned}$$

We also give the moisture content  $\theta$  a Hermite cubic representation. To do this, we need expressions for the nodal values of the derivatives  $\partial\theta/\partial x$ ,  $\partial\theta/\partial y$ , and  $\partial^2\theta/\partial x \partial y$ . Since physically  $\theta$  is an explicit function of  $h$ , we must use the chain rule to express spatial derivatives of  $\theta$  in terms of the nodal spatial derivatives  $h_i^{(x)}$ ,  $h_i^{(z)}$ , and  $h_i^{(xz)}$ . We thus obtain the cubic expansion

$$\begin{aligned} \hat{\theta}(\mathbf{x}) &= \sum_{i=1}^{MN} \left\{ \theta(h_i) \varphi_{00i}(\mathbf{x}) + \frac{d\theta}{dh}(h_i) h_i^{(x)} \varphi_{10i}(\mathbf{x}) \right. \\ &\quad + \frac{d\theta}{dh}(h_i) h_i^{(z)} \varphi_{01i}(\mathbf{x}) \\ &\quad \left. + \left[ \frac{d^2\theta}{dh^2}(h_i) h_i^{(x)} h_i^{(z)} + \frac{d\theta}{dh}(h_i) h_i^{(xz)} \right] \varphi_{11i}(\mathbf{x}) \right\} \end{aligned}$$

This  $C^1$  projection of  $\theta$  parallels the successful one-dimensional calculations reported in our earlier paper [Allen and Murphy, 1985]. It is worth mentioning here that numerical experiments with less expensive, lower-order discretizations of  $\theta$ , using, for example,  $C^0$  linear projections, failed to yield stable solution schemes. We do not know the precise reason for the instability. However, observe that a cubic expansion of  $\theta$  allows the accumulation term  $(\hat{\theta}^{n+1} - \hat{\theta}^n)/\Delta t$  to match more closely the polynomial degrees of other terms in the finite-element expansion of (3).

Finally, for the coefficients  $K$  and  $d\theta/dh$  in (3) we adopt piecewise bilinear approximations:

$$\hat{K}(\mathbf{x}) = \sum_{i=1}^{MN} K(h_i) L_i(x) L_i(z)$$

$$\left( \frac{d\theta}{dh} \right)^\wedge(\mathbf{x}) = \sum_{i=1}^{MN} \frac{d\theta}{dh}(h_i) L_i(x) L_i(z)$$

where  $L_i$  is just the one-dimensional piecewise linear Lagrange (chapeau) basis function associated with node  $i$ . On the grid  $\{\zeta_1 < \dots < \zeta_L\}$  defined above,

$$\begin{aligned} L_i(\zeta) &= (\zeta - \zeta_{i-1}) / \Delta\zeta & \zeta \in [\zeta_{i-1}, \zeta_i] \\ L_i(\zeta) &= (\zeta_{i+1} - \zeta) / \Delta\zeta & \zeta \in [\zeta_i, \zeta_{i+1}] \\ L_i(\zeta) &= 0 & \text{otherwise} \end{aligned}$$

Here, in contrast to the moisture content  $\theta$ , the use of  $C^0$  projections seems to impose no difficulties with stability. In

fact, one might argue that low-degree polynomial approximations are desirable here, since in (3) the coefficients  $K$ ,  $\nabla K$ , and  $d\theta/dh$  all multiply functions whose finite-element representations have higher degrees. The use of Lagrange bilinear polynomials for these variables avoids possible oscillatory behavior associated with high-degree interpolation by guaranteeing that each term in the finite-element projection of (3) has local degree four or less.

Substituting all of these finite-element projections into (3) yields a temporally discrete scheme with a finite number of unknown nodal degrees of freedom at each iteration of each time step.

### 3. COLLOCATION SOLUTION SCHEME

To determine the nodal values of  $\delta\hat{h}$  and therefore advance the head  $\hat{h}$  in time, we need a set of algebraic equations at each iterative step. Some of these equations come from boundary conditions; the rest we shall construct using finite-element collocation. Let us begin by reviewing the boundary conditions. We shall encounter two types of boundary data: Dirichlet data, prescribing the head  $h(\mathbf{x}, t)$  along a boundary segment  $\partial\Omega_D \subset \partial\Omega$ , and Neumann data, prescribing the outward normal derivative  $\nabla h(\mathbf{x}, t) \cdot \mathbf{n}(\mathbf{x}, t)$  along another, disjoint boundary segment  $\partial\Omega_N \subset \partial\Omega$ . We shall not encounter Robin boundary data, so we assume  $\partial\Omega_D \cup \partial\Omega_N = \partial\Omega$ .

Collocation differs from standard Galerkin techniques in its treatment of boundary conditions. Viewed as a method of weighted residuals, collocation yields integral equations of the form

$$\int_{\Omega} [\hat{\mathcal{A}}^{n+1,m} \delta h + \mathcal{R}(\hat{h}^{n+1,m})] \delta(\mathbf{x} - \bar{\mathbf{x}}_k) d\mathbf{x} = 0 \quad (5)$$

Here  $\hat{\mathcal{A}}$  signifies the analog of the operator  $\mathcal{A}$  computed using finite-element representations of its coefficients, and  $\delta(\mathbf{x} - \bar{\mathbf{x}}_k)$  is a Dirac distribution centered at some point  $\bar{\mathbf{x}}_k \in \Omega$ . While these equations are formally similar to those arising in the classic Galerkin method, the use of the singular distributions  $\delta(\mathbf{x} - \bar{\mathbf{x}}_k)$  as weighting functions prohibits the use of Green's theorem to rewrite the integral of the first term. Therefore no boundary integral arises, and hence there is no way to accommodate Neumann conditions naturally. For this reason, the finite-element collocation formulation requires that both Dirichlet and Neumann data be treated as essential boundary data. We must therefore incorporate all boundary information into our trial functions in advance of collocating.

By using the tensor-product basis defined above, we have tacitly oriented the computational boundaries parallel to the coordinate axes. In this frame the outward unit normal vector  $\mathbf{n}$  and unit tangent vector  $\boldsymbol{\tau}$  to  $\partial\Omega$  will be  $\pm\mathbf{e}_x$  or  $\pm\mathbf{e}_z$ , depending on position along  $\partial\Omega$ . Suppose  $\mathbf{x}_i \in \partial\Omega_D$ . Then  $\hat{h}^{n+1}(\mathbf{x}_i) = h_i^{n+1}$  is a fixed, known quantity, and therefore  $\delta_i = 0$ . Moreover, we can differentiate the boundary data tangentially along  $\partial\Omega_D$  to deduce fixed values for  $\nabla\hat{h}^{n+1} \cdot \boldsymbol{\tau}$ , thus forcing  $\delta_i^{(x)} = 0$  if  $\boldsymbol{\tau} = \pm\mathbf{e}_x$  and  $\delta_i^{(z)} = 0$  if  $\boldsymbol{\tau} = \pm\mathbf{e}_z$ . Similarly, if  $\mathbf{x}_i \in \partial\Omega_N$ , then  $\nabla\hat{h}^{n+1}(\mathbf{x}_i)$  is a fixed, known quantity, forcing  $\delta_i^{(x)} = 0$  if  $\mathbf{n} = \pm\mathbf{e}_x$  and  $\delta_i^{(z)} = 0$  if  $\mathbf{n} = \pm\mathbf{e}_z$ . Differentiating the boundary data tangentially in this case will give fixed values for  $\nabla(\nabla\hat{h}^{n+1} \cdot \mathbf{n}) \cdot \boldsymbol{\tau}$  along  $\partial\Omega_N$ , forcing  $\delta_i^{(xz)} = 0$ . Therefore at any boundary node within a boundary line segment the boundary data determine two nodal parameters. At corner nodes of the rectangle  $\Omega$  the boundary data along the intersecting boundary edges will combine to determine three nodal parameters.

To determine the remaining boundary and interior nodal

parameters, we impose the weighted-residual criterion (5) at a set of collocation points  $\bar{\mathbf{x}}_k \in \Omega$ . This yields a system of linear algebraic equations each having the form

$$\left[ -\frac{1}{\Delta t} \frac{d\hat{\theta}^{n+1,m}}{dh}(\bar{\mathbf{x}}_k) + \hat{K}^{n+1,m}(\bar{\mathbf{x}}_k) \left( \frac{\partial^2}{\partial x^2} + \frac{\partial^2}{\partial z^2} \right) + \frac{\partial \hat{K}^{n+1,m}}{\partial x}(\bar{\mathbf{x}}_k) \frac{\partial}{\partial x} + \frac{\partial \hat{K}^{n+1,m}}{\partial z}(\bar{\mathbf{x}}_k) \frac{\partial}{\partial z} \right] \delta\hat{h}(\bar{\mathbf{x}}_k) = -\hat{R}^{n+1,m}(\bar{\mathbf{x}}_k) \quad (6)$$

where  $\hat{R}$  represents the expression obtained by substituting the appropriate interpolatory projections for the spatially varying quantities in the functional  $\mathcal{R}(\hat{h})$ .

We choose for the collocation points  $\bar{\mathbf{x}}_k$  the Gauss points associated with four-point quadrature on each rectangular element  $[x_p, x_{p+1}] \times [z_q, z_{q+1}]$  [Pinder *et al.*, 1978]. If we imagine such an element mapped onto the square  $[-1, 1] \times [-1, 1]$  in a "local"  $(\xi, \eta)$  coordinate system defined by  $\xi = (2x - 2x_p - \Delta x)/\Delta x$ ,  $\eta = (2z - 2z_q - \Delta z)/\Delta z$ , then the collocation points  $\bar{\mathbf{x}}_k$  in the element have images whose coordinates are  $(\bar{\xi}_k, \bar{\eta}_k) = (\pm 1/\sqrt{3}, \pm 1/\sqrt{3})$ . Given the assignment of boundary data described above, this choice of collocation points furnishes exactly the right number of additional equations for the remaining unknown nodal parameters and gives optimal  $\mathcal{O}(\Delta x^4 + \Delta z^4)$  accuracy estimates for the linearized problem at each time step [Prenter and Russell, 1976].

For any collocation point  $\bar{\mathbf{x}}_k$  from the set just defined, (6) yields a linear equation involving the unknown coefficients of  $\delta\hat{h}$  at the four nodes surrounding  $\bar{\mathbf{x}}_k$ . If we denote the vector containing all such coefficients, listed lexicographically, as  $\boldsymbol{\delta}$ , call the matrix of coefficients in the collocation equations  $\mathbf{A}^{n+1,m}$ , and let  $\mathbf{R}^{n+1,m}$  stand for the vector of residual values  $\hat{R}^{n+1,m}(\bar{\mathbf{x}}_k)$ , then we see that (6) reduces to a matrix equation  $\mathbf{A}^{n+1,m} \boldsymbol{\delta} = -\mathbf{R}^{n+1,m}$  at each iteration.

The discretization procedure just described yields the following iterative algorithm for advancing the approximate solution from  $t = n\Delta t$  to  $t = (n+1)\Delta t$ .

1. Let  $n \leftarrow n + 1$ ,  $m \leftarrow 0$ ,  $\hat{h}^{n+1,0}(\mathbf{x}) \leftarrow \hat{h}^n(\mathbf{x})$ .
2. Compute the residual vector  $\mathbf{R}^{n+1,m}$ .
3. If  $\|\mathbf{R}^{n+1,m}\|_{\infty} < \epsilon$ , then  $\hat{h}^{n+1,m}(\mathbf{x})$ . Go to step 1.
4. Compute the matrix  $\mathbf{A}^{n+1,m}$ .
5. Solve  $\mathbf{A}^{n+1,m} \boldsymbol{\delta} = -\mathbf{R}^{n+1,m}$  for the coefficients of  $\delta\hat{h}(\mathbf{x})$ .
6. Let  $\hat{h}^{n+1,m+1}(\mathbf{x}) \leftarrow \hat{h}^{n+1,m}(\mathbf{x}) + \delta\hat{h}(\mathbf{x})$ .
7. Go to step 2.

### 4. SAMPLE PROBLEMS

To show the effectiveness of our collocation scheme, we solve two sample problems. The first is essentially a one-dimensional vertical infiltration problem solved using a two-dimensional spatial grid. The purpose of this exercise is to allow comparisons with solutions generated by one-dimensional formulations known to be accurate. The one-dimensional equation is

$$\frac{\partial}{\partial z} \left( K \frac{\partial h}{\partial z} \right) - \frac{\partial K}{\partial z} - \frac{\partial \theta}{\partial t} = 0 \quad z \in (0, 1 \text{ m})$$

with boundary conditions

$$h(0, t) = -0.14495 \text{ m}$$

$$\frac{\partial h}{\partial z}(1 \text{ m}, t) = 0$$

The initial condition, stated in terms of moisture content  $\theta$ , is

$$\theta(h(z, 0)) = 0.15 + z/12 \quad \text{if } 0 < z \leq 0.6 \text{ m}$$

$$\theta(h(z, 0)) = 0.2 \quad \text{if } 0.6 \text{ m} < z < 1 \text{ m}$$

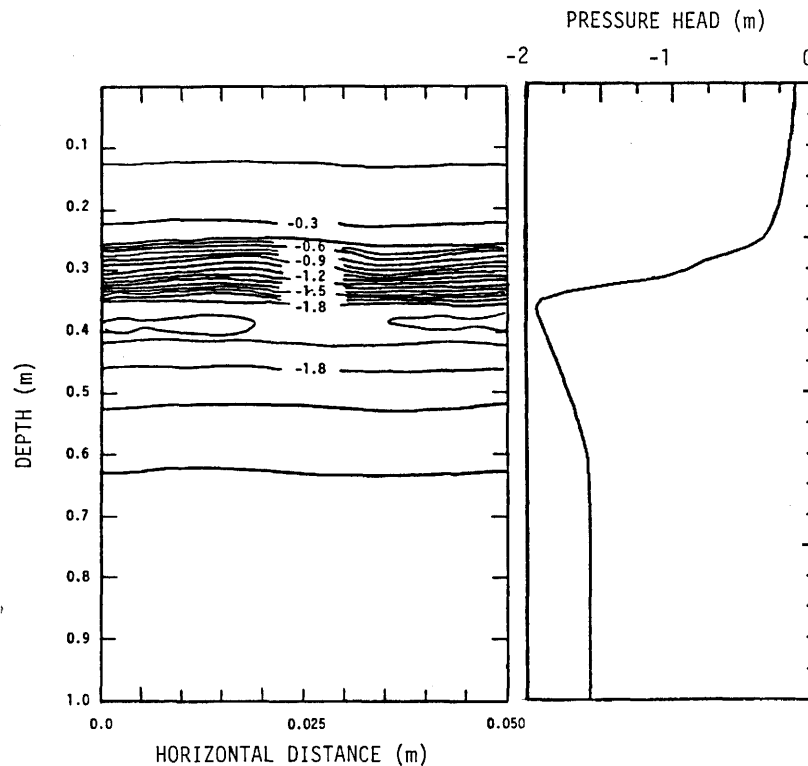


Fig. 1. Comparison of solutions for a vertical infiltration problem at 2 hours, using the two-dimensional collocation formulation (left) and a mass-conserving one-dimensional scheme (right).

This equation amounts to a condition on  $h$  given the functional relationship

$$\theta(h) = 0.6829 - 0.09524 \ln |100h| \quad \text{if } h \leq -0.29484 \text{ m}$$

$$\theta(h) = 0.4531 - 0.02732 \ln |100h| \quad \text{if } h > -0.29484 \text{ m}$$

To complete the statement of the problem, we use

$$K(h) = 1.157 \times 10^{-7} (19.34 \times 10^5 |100h|^{-3.4095}) \text{ m/s} \quad h \leq -0.29484 \text{ m}$$

$$K(h) = 1.157 \times 10^{-7} (516.8 |100h|^{-0.97814}) \text{ m/s} \quad h > -0.29484 \text{ m}$$

for the hydraulic conductivity.

This problem is the same as that posed by Warrick *et al.* [1971], except that we express the constitutive relationships in SI units. The solution appears in the literature in several places, including a paper by van Genuchten [1982], who compares various numerical solutions with a quasi-analytic solution developed by Philip [1957], and our earlier paper [Allen and Murphy, 1985], where we discuss a mass-conserving one-dimensional scheme.

To test the two-dimensional collocation scheme against this problem, we solve the analogous problem

$$\nabla \cdot (K \nabla h - \mathbf{e}_z) - \frac{\partial \theta}{\partial t} = 0 \quad \mathbf{x} \in (0, 0.05 \text{ m}) \times (0, 1 \text{ m})$$

$$h(x, 0, t) = -0.14495 \text{ m}$$

$$\frac{\partial h}{\partial z}(x, 1 \text{ m}, t) = 0$$

$$\frac{\partial h}{\partial x}(0, z, t) = \frac{\partial h}{\partial x}(0.05 \text{ m}, z, t) = 0$$

with the same initial conditions as above imposed uniformly in the  $x$  direction. The boundary data along the vertical sides of the spatial domain imply no horizontal flux across these boundaries. We use a two-dimensional grid in which  $\Delta x = \Delta z = 0.05 \text{ m}$  and a time step  $\Delta t = 60 \text{ s}$ , imposing a residual tolerance  $\varepsilon = 10^{-5} \text{ s}^{-1}$ .

Figure 1 shows the level curves of  $h$  at 2 hours. Alongside this plot stands a profile of  $h$  at 2 hours computed using our one-dimensional collocation code [Allen and Murphy, 1985]. This latter solution agrees very closely with those of van Genuchten [1982] and Philip [1957]. The plots in Figure 1 show excellent agreement between the two formulations, both in the values of the pressure head and in the location of the wetting front.

Our second sample problem is similar to one solved by van Genuchten [1983] using a Galerkin procedure on Hermite bicubics. This problem describes water infiltrating from a source located 0.15 m below the soil surface. The governing differential equation is

$$\nabla \cdot [K(\nabla h - \mathbf{e}_z)] - \frac{\partial \theta}{\partial t} + Q = 0$$

where  $Q$  is the water source, measured in  $\text{s}^{-1}$ . The spatial domain of the problem is  $\Omega = (0, 0.61 \text{ m}) \times (-3.5 \text{ m}, 0)$ . We assume that the left side  $\{0\} \times (-3.5 \text{ m}, 0)$  and right side  $\{0.61 \text{ m}\} \times (-3.5 \text{ m}, 0)$  are lines of symmetry with no normal flux, that the bottom  $(0, 0.61 \text{ m}) \times \{-3.5 \text{ m}\}$  is a free-draining boundary and that the soil surface  $(0, 0.61 \text{ m}) \times \{0\}$  remains at atmospheric pressure. These assumptions lead to the mixed boundary conditions

$$\frac{\partial h}{\partial x}(0, z, t) = \frac{\partial h}{\partial x}(0.61 \text{ m}, z, t) = 0 \quad -3.5 \text{ m} < z < 0, t > 0$$

$$\frac{\partial h}{\partial z}(x, -3.5 \text{ m}, t) = 0 \quad 0 < x < 0.61 \text{ m}, t > 0$$

$$h(x, 0, t) = -0.14495 \text{ m} \quad 0 < x < 0.61 \text{ m}, t > 0$$

We impose the initial condition  $h(x, 0) = -0.387 \text{ m}$ ,  $x \in \Omega$ . For the material properties  $K$  and  $\theta$  we assume the same functional forms as van Genuchten, which in SI units are

$$K(h) = (1.157 \times 10^{-7})[96.768 \exp(12.58h)] \text{ m/s} \quad h \leq 0$$

$$\theta(h) = 0.10 + 0.40/[1 + 0.0025(100h)^2]^{1/2} \quad h \leq 0$$

We assume a point source of the form  $Q(x) = Q_0\delta(x - 0)\delta(z + 0.15 \text{ m})$  with a source strength  $Q_0 = 5 \times 10^{-5} \text{ s}^{-1}$ . In finite-element collocation we must approximate  $Q$  by a square-integrable function. This requirement contrasts with classical Galerkin procedures, where the integrability of the test functions permits us to use singular distributions like the Dirac  $\delta$  in modeling point sources in the operator equation. We therefore choose a piecewise bilinear approximation of the form

$$\hat{Q}(x) = \sum_{i=1}^{MN} Q_i L_i(x) L_i(z)$$

where the point  $x_i^{\text{source}} = (0, -0.15 \text{ m})$  is a node,  $Q_i = 0$  if  $x_i \neq x_i^{\text{source}}$ , and  $\int_{\Omega} \hat{Q} \, dx = \int_{\Omega} Q \, dx$ .

We solve the resulting collocation equations on the five-element-by-eleven-element grid given in the work by van Genuchten [1983] using a time step  $\Delta t = 3600 \text{ s}$  (one hour). Figure 2 shows the structure of the matrix  $A$  that has to be inverted at each iteration in the nonlinear time-stepping procedure. The bandwidth for this matrix is 31. We use a direct solver executing LU factorization with partial pivoting on banded asymmetric matrices.

Figure 3 shows the spatial variation of  $\hat{h}(x, t)$  at 2, 6, and 12 hours. At 2 hours the source already has a noticeable effect on the pressure head. In the horizontal direction  $\hat{h}$  peaks at the source, drops off, and then levels out. In the vertical direction the pressure head gradually increases further down into the

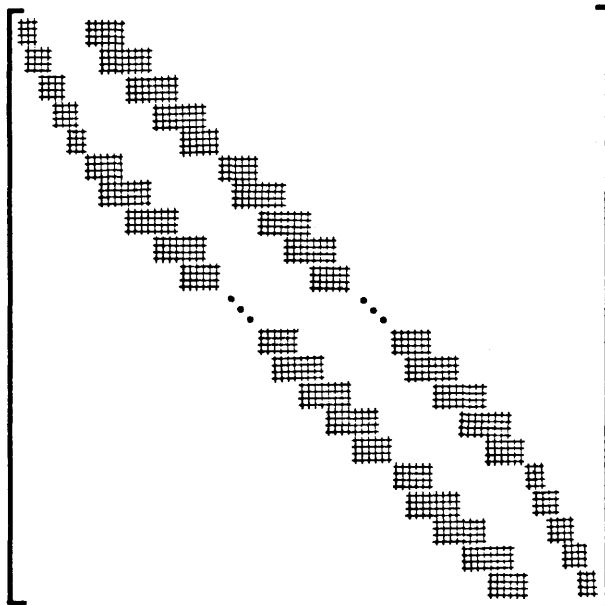


Fig. 2. Matrix structure for the irrigation problem.

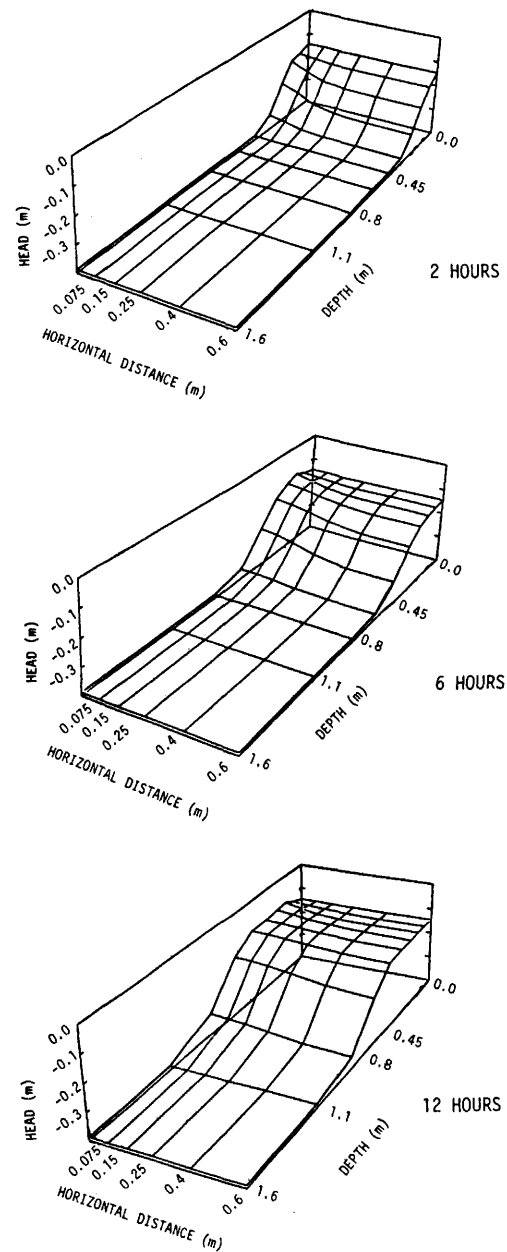


Fig. 3. Pressure head solution at 2, 6, and 12 hours for the irrigation problem.

column as time progresses. Finally, at  $t = 12$  hours  $\hat{h}$  reaches a very close approximation to the steady state solution in the sense that this solution is virtually identical to solutions at later times.

It is also interesting to note the effects of our approximations to the Newton method on the convergence of the iterative scheme. Ordinarily, if we had used the exact Fréchet derivative of the time-differenced operator  $\mathcal{R}$  in (2), we would expect the iterative scheme to converge quadratically at each time step. Figure 4, however, shows that plots of  $\ln \|\hat{R}^{n+1,m+1}\|_{\infty}$  versus  $\ln \|\hat{R}^{n+1,m}\|_{\infty}$  typically exhibit straight-line trends with slopes not far from unity. Thus the approximations used in constructing the iterative scheme apparently slow the convergence to a linear rate. This finding may deserve some more careful analysis in the future.

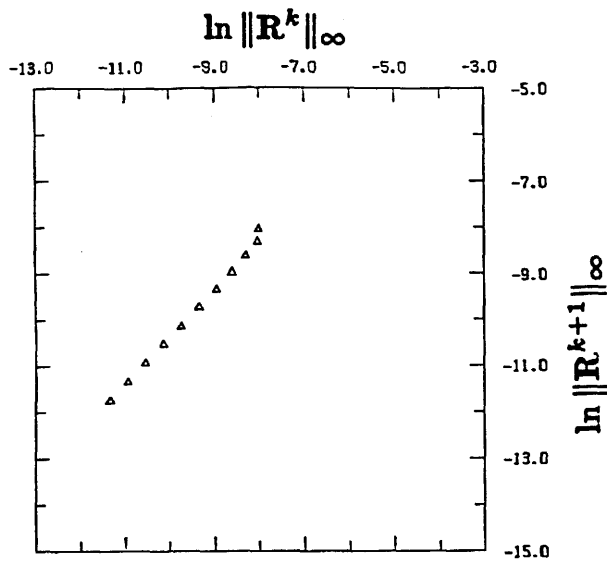


Fig. 4. Logarithmic plot of successive residual norms in the Newton-like iterative scheme. Line of least squares fit has slope 1.14.

### 5. CONCLUSION

The finite-element collocation method produces good approximations to pressure head distributions in unsaturated flows through porous media. As we have shown, the mass-conserving iterative formulation, demonstrated earlier for one-dimensional flows, extends in a natural way to two space dimensions. One area deserving further investigation is the linear algebra involved at each iterative stage. Since the matrices for the multidimensional problems have an asymmetric block structure without diagonal dominance, better methods for solving the linear iterative systems would be a boon to further applications. A particularly promising approach along these lines is that of Celia and Pinder [1986], who advance an alternating-direction collocation scheme that reduces two-dimensional problems to sequences of one-dimensional problems. Given the efficiencies in matrix assembly already inherent in finite-element collocation, this general area of inquiry has the potential to make collocation even more competitive with Galerkin techniques.

*Acknowledgments.* The Wyoming Water Research Center provided partial support for this work. The National Science Foundation

also provided support through grants CEE-8404266 and DMS-8504360.

### REFERENCES

- Allen, M. B., and C. L. Murphy, A finite-element collocation technique for variably saturated flows in porous media, *Numer. Meth. PDEs*, 3, 229-239, 1985.
- Celia, M. A., and G. F. Pinder, An alternating-direction collocation solution for the unsaturated flow equation, in *Proceedings Sixth International Conference on Finite Elements in Water Resources*, edited by A. Sa da Costa et al., CML Publications, Southampton, United Kingdom, 1986.
- Milly, P. C. D., A mass-conservative procedure for timestepping in models of unsaturated flow, in *Proceedings Fifth International Conference on Finite Elements in Water Resources*, edited by J. P. Laible et al., pp. 103-112, Springer-Verlag, New York, 1984.
- Murphy, C. L., and M. B. Allen, A collocation model of two-dimensional unsaturated flow, in *Proceedings Sixth International Conference on Finite Elements in Water Resources*, edited by A. Sa da Costa et al., CML Publications, Southampton, United Kingdom, 1986.
- Philip, J. R., Numerical solution of equations of the diffusion type with diffusion concentration dependent, II, *Aust. J. Phys.*, 10, 29-42, 1957.
- Pinder, G. F., E. O. Frind, and M. A. Celia, Groundwater flow simulation using collocation finite elements, in *Proceedings Second International Conference on Finite Elements in Water Resources*, edited by C. A. Brebbia et al., pp. 1.171-1.185, Pentech, London, 1978.
- Prenter, P. M., *Splines and Variational Methods*, John Wiley, New York, 1976.
- Prenter, P. M., and R. Russell, Orthogonal collocation for elliptic partial differential equations, *SIAM J. Numer. Anal.*, 13, 923-939, 1976.
- Richards, L. A., Capillary conduction of liquids in porous media, *Physic. J.*, 318-333, 1931.
- Van Genuchten, M.Th., A comparison of numerical solutions of the one-dimensional unsaturated-saturated flow and mass transport equations, *Adv. Water Resour.*, 5, 47-55, 1982.
- Van Genuchten, M.Th., An Hermitian finite element solution of the two-dimensional saturated-unsaturated flow equation, *Adv. Water Resour.*, 6, 106-111, 1983.
- Warrick, A. W., J. W. Biggar, and D. R. Nielsen, Simultaneous solute and water transfer for unsaturated soil, *Water Resour. Res.*, 7, 1216-1225, 1971.
- M. B. Allen, Department of Mathematics, The University of Wyoming, Box 3036, University Station, Laramie, WY 82071.
- C. L. Murphy, 6510 TESTW/TEXTS, Edwards Air Force Base, CA 93523.

(Received May 20, 1986;  
accepted May 29, 1986.)